Inorganic Chemistry
Article
pubs.acs.org/IC

Porous Metal−Organic Framework Catalyzing the Three-Component Coupling of Sulfonyl Azide, Alkyne, and Amine

Tao Yang, Hao Cui, Changhe Zhang, Li Zhang,* and Cheng-Yong Su*

MOE Laboratory of Bioinorganic and Synthetic Chemistry/KLGHEI of Environment and Energy Chemistry, State Key Laboratory of Optoelectronic Materials and Technologies, School of Chemistry and Chemical Engineering, Sun Yat-sen University, Guangzhou 510275, P.R. China

Supporting Information

ABSTRACT: The robustly porous metal−organic framework MOF−Cu_2I_2(BTTP4) (BTTP4 = benzene-1,3,5-triyl triisonicotinate) was shown to work as an efficiently heterogeneous catalyst for the three-component coupling of sulfonyl azides, alkynes, and amines, leading to the formation of *N*-sulfonyl amidines in good yields. MOF−Cu_2I_2(BTTP4) can be recycled by simple filtration and reused at least four times without any loss in yield. Studies of the ligand effects on the three-component coupling reactions showed that BTTP4 could enhance the rate, as well as the chemoselectivity, when aromatic alkynes were employed. The catalytic process has been thoroughly studied by means of single-crystal and powder X-ray diffraction, gas and solvent adsorption, in situ ^1H NMR and FT-IR spectroscopy, X-ray photoelectron spectra (XPS), and ICP analysis of Cu leaching.

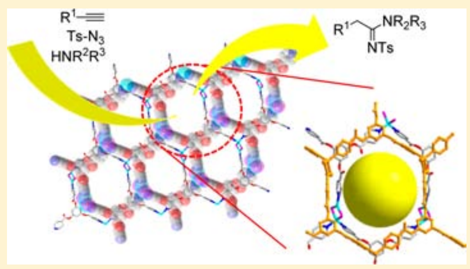

1. INTRODUCTION

In the past decade, crystalline metal−organic frameworks (MOFs), also called porous coordination polymers (PCPs), have attracted considerable interest due to their intrinsic properties such as high internal surface area and micro/meso porosity. They are regarded as promising porous materials that are able to mimic zeolite catalysts with specific shape- and/or size-selectivity. Since the 1990s, a large number of MOFs have been examined as heterogeneous catalysts.[1−8] Among many strategies for synthesizing catalytic MOFs, direct incorporation of a homogeneous catalyst into a linker ligand and the grafting of an organocatalyst onto a metal node have become the most promising approaches toward efficiently building hetereogeneous catalysts.[9−15] Within both strategies, the metal nodes are the building units rather than the catalytic sites.

We are interested in the development of catalytic MOFs, in which the metal nodes can act as the catalytic sites and promote the reactions leading to the formation of valuable products.[16−24] We found that the Cu^I ion is an adequate metal candidate, which prefers to generate coordination hosts with low coordination numbers (usually from 2- to 3-coordination), while allowing additional metal−guest interactions due to its flexible coordination environment (up to 5).[25−27] Its potential redox activity is essential for a variety of catalytic reactions. Therefore, construction of porous CuI−MOFs may provide a convenient approach to heterogeneously self-support catalysts with Cu^I ions acting as both metal nodes and catalytic sites. CuI also plays an important role in many conventional catalytic reactions, especially in the remarkable click reactions[28,29] and the multicomponent coupling reactions.[30−33] On the other hand, careful investigations into catalytic activity, as well as detailed mechanistic studies, show that nitrogen-containing ligands such as benzimidazole, triazole, and pyridine could accelerate CuI-catalyzed reactions.[34,35] Taking these considerations into account, we are interested in the self-assembly of CuI−MOFs using commercially available CuI and *N*-heterocyclic tripodal ligands with the desire to develop porous MOFs potentially possessing ligand-accelerated catalytic activity.

In light of this strategy, our group recently developed a robust, porous CuI-based MOF, Cu_2I_2(BTTP4) (BTTP4 = benzene-1,3,5-triyl triisonicotinate, hereafter designated as MOF−Cu_2I_2(BTTP4)).[25] After fully characterizing this MOF by single-crystal X-ray crystallography, thermogravimetry and variable-temperature powder X-ray diffraction (PXRD), and gas/vapor adsorption, we believe that MOF−Cu_2I_2(BTTP4) could be an ideal MOF structural model (Figures 1 and S1) for application in heterogeneous catalysis due to the following considerations: (i) it has a large free volume of 1776.9 $Å^3$, which amounts to 43% of the unit cell volume; (ii) it has large one-dimensional channels (9 × 12 $Å^2$) after considering the van der Waals radii, which can be completely evacuated to leave permanent porosity for guest molecule access; (iii) the metal core is a Cu_2I_2 cluster, which contains one four-coordinating CuI center in a CuI_2N_2 tetrahedral geometry and one three-coordinating CuI center in a CuI_2N trigonal geometry, providing an unsaturated metal site to be exposed in the cavity for potential catalytic reactions; and (iv) the empty framework has been proven to preferentially include aromatic guests over nonaromatics easily through a solid-solution diffusion/exchange process. These features may make MOF−Cu_2I_2(BTTP4) a

Received: May 16, 2013
Published: July 25, 2013

   dx.doi.org/10.1021/ic4012229 | Inorg. Chem. 2013, 52, 9053−9059

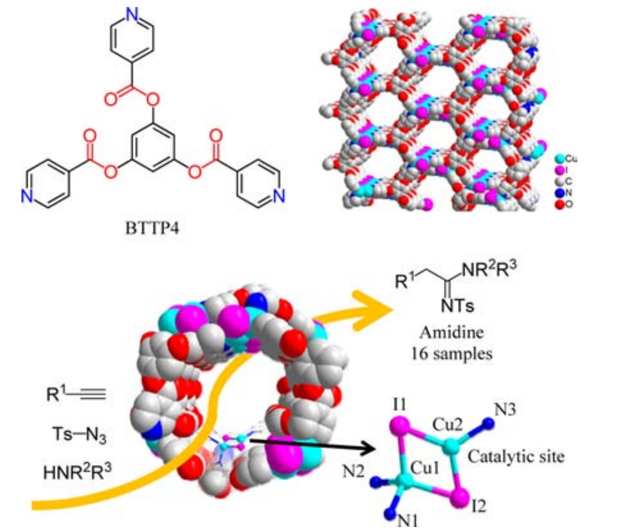

Figure 1. Molecular structure of the ligand BTTP4, 1D channels in MOF−Cu_2I_2(BTTP4), and representation of catalytic behaviors.

platform to carry out reactions in the framework channels and to display shape- and/or size-selective catalytic capability. Herein, we employ MOF−Cu_2I_2(BTTP4) to the three-component coupling reactions of sulfonyl azides, alkynes, and amines (Figure 1).[30] To the best of our knowledge, this is the first report of the application of a MOF catalyst into the synthesis of amidines.

2. EXPERIMENTAL SECTION

2.1. General Information. All the reagents in the present work were obtained from the commercial source and used directly without further purification. Infrared spectra on KBr pellets were collected with a Nicolet/Nexus-670 FT-IR spectrometer in the region of 400−4000 cm^{-1}. ^{1}H NMR spectra were recorded with a Varian Mercury Plus 300 MHz spectrometer. The X-ray powder diffraction patterns were measured on a Bruker D8 Advance diffractometer at 40 kV and 40 mA with a Cu target tube and a graphite monochromator. The sorption isotherms for CO_2 (195 K) gas and CH_3OH (298 K) vapor were measured with a Micromeritics ASAP 2020 gas sorption analyzer. Prior to the sorption examination, the samples are vacuumed at 35 °C for 16 h. Synthesis of MOF−Cu_2I_2(BTTP4) was completed according to our previous procedure.[25]

2.2. Typical Procedure for the Three-Component Coupling Reactions Catalyzed by MOF−Cu_2I_2(BTTP4). To CH_3CN (1 mL) in a vessel (10 mL) were added MOF−Cu_2I_2(BTTP4) (10 mg, 0.012 mmol), phenylacetylene (51.0 mg, 0.5 mmol), and tosyl azide (118 mg, 0.6 mmol). Then, diisopropylamine (60.6 mg, 0.6 mmol) was added slowly to the above vessel. The whole reaction mixture was allowed to stand at room temperature for 2 h. After that, the supernatant was filtered through a thin pad of Celite and was concentrated to dryness, which was followed by a flash chromatography. A pure product of *N,N*-diisopropyl-2-phenyl-*N*′-tosylacetimidamide (**1a**) was obtained as an off-white solid (163.3 mg, 88%). R_f = 0.66 (EtOAc/hexane = 1/2). ^{1}H NMR (300 MHz, $CDCl_3$) δ: 7.82 (d, *J* = 8.3 Hz, 2H), 7.31−7.18 (m, 7H), 4.41 (s, 2H), 3.97 (dt, *J* = 13.2, 6.7 Hz, 1H), 3.48−3.43 (m, 1H), 2.40 (s, 3H), 1.41 (d, *J* = 6.8 Hz, 6H), 0.89 (d, *J* = 6.6 Hz, 6H). IR (KBr, ν, cm^{-1}): 2973, 2930, 1542, 1458, 1443, 1374, 1262, 1137, 1083, 754, 546 cm^{-1}. MS (ESI) *m/z*: calcd for $C_{21}H_{29}N_2O_2S$ $[M + H]^+$ 373.19; found, 373.11.

2.3. Procedure for the Three-Component Coupling Reactions Monitored by In Situ ^{1}H NMR. To a NMR tube were added 0.006 mmol MOF−Cu_2I_2(BTTP4) (or CuI), phenylacetylene (25.5 mg, 0.25 mmol), tosyl azide (59.3 mg, 0.3 mmol), diisopropylamine (30.3 mg, 0.3 mmol), and CD_3CN (0.5 mL). The conversion of the reaction (based on phenylacetylene) was monitored by ^{1}H NMR every 10 min.

3. RESULTS AND DISCUSSION

3.1. Catalytic Performances of MOF−Cu_2I_2(BTTP4). Recently, Chang and co-workers discovered that CuI can promote three-component coupling of sulfonyl azides, alkynes, and amines to generate *N*-sulfonyl amidines, which are prominent structural motifs in numerous natural bioactive products.[30] Encouraged by this important finding, we were interested in exploring if the MOF−Cu_2I_2(BTTP4) can be used to promote the three-component coupling in a heterogeneous way. Compared to the conventional heterogeneous catalysts based on polymer supports, self-supported porous MOFs as heterogeneous catalysts are expected to display superior shape- and/or size-selectivity because they provide a platform to carry out catalytic reactions within their cavities.[1−7] According to our previous adsorption and guest exchange studies, MOF−Cu_2I_2(BTTP4) exhibited good gas and solvent adsorptive capacity and facile aromatic guest inclusion behavior, and it had the capability to take in two aromatic molecules such as benzene, toluene, and ethylbenzene per Cu_2I_2 unit through a diffusion/exchange process via the solid-solution interface.[25] This paves the way for testing the catalytic capability of MOF−Cu_2I_2(BTTP4) in the three-component coupling reactions, especially for those with aromatic alkynes. To our delight, a series of aromatic alkynes can take part in the catalytic reactions (entries 1−7, Table 1). It is noted that due to the highest stability of MOF−Cu_2I_2(BTTP4) in CH_3CN, we herein chose CH_3CN as the reaction media rather than THF because it was proven to be the best solvent for naked CuI-catalyzed reactions.[30] In all cases, *N*-tosylamidines were formed as the sole products, whereas tosyltriazoles have not been detected. Chang and Fokin discovered that tosyltriazoles might become the major products when the CuI-catalyzed reactions occurred at lower temperature (e.g., 0 °C) in $CHCl_3$ and in the absence of amines.[36] We also found that if the CuI-catalyzed three-component coupling reaction among tosylazide (Ts−N_3), phenylacetylene (PhCCH), and diisopropylamine ((*i*-Pr)$_2$NH) proceeded in 1:1 $CH_3CN/CHCl_3$, the chemoselectivity of *N*-tosylaldimine (**1a**) and tosyltriazole (**1b**) was changed to 3:1 (more information will be discussed in the next section). The molecular structures of amidines **1a** and **4a** have been unambiguously determined by single-crystal X-ray crystallographic analyses, which disclosed an *E*-form of the generated C═N double bond (Figures S11 and S12), the same as the transformation catalyzed by naked CuI.[30]

For comparison, *N*-tosylamidines were obtained with modest yields from the reactions with alkyl alkynes (entries 8−12). Especially, the yields of **10−12a** were less than 60%, which were obtained from the bulky alkynes (entries 10−12). In contrast, the corresponding amidines in the CuI-catalyzed reactions were isolated in high yields.[30] For example, **10a** was obtained with 79% yield from the CuI-catalyzed reaction, compared to a lower yield (51%, entry 10) in the presence of MOF−Cu_2I_2(BTTP4).

We monitored the process of the catalytic transformations with the preferable aromatic alkyne PhCCH over the less-favored aliphatic alkyne *t*-BuCCH by in situ ^{1}H NMR, as shown in Figures 2 and S6−9. For comparison purposes, we also monitored the process catalyzed by naked CuI. As shown in Figure 2, in the presence of MOF−Cu_2I_2(BTTP4), the reactions of PhCCH and *t*-BuCCH started with almost the

Table 1. Three-Component Coupling Reactions of Sulfonyl Azide, Alkyne, and Amine Catalyzed by MOF−Cu_2I_2(BTTP4)[a]

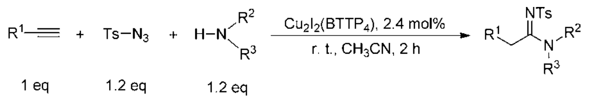

Entry	Alkyne	HNR^2R^3	Product	Isolated Yield/%
1	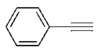	(*i*-Pr)$_2$NH	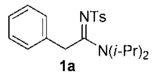 1a	88
2	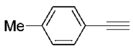	(*i*-Pr)$_2$NH	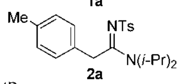 2a	90
3	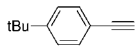	(*i*-Pr)$_2$NH	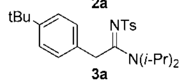 3a	88
4	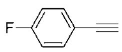	(*i*-Pr)$_2$NH	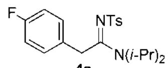 4a	61
5	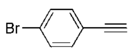	(*i*-Pr)$_2$NH	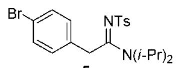 5a	86
6	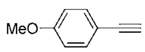	(*i*-Pr)$_2$NH	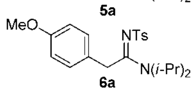 6a	89
7	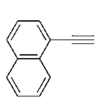	(*i*-Pr)$_2$NH	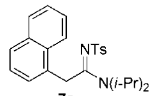 7a	65
8	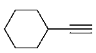	(*i*-Pr)$_2$NH	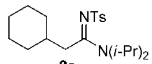 8a	65
9	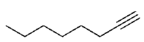	(*i*-Pr)$_2$NH	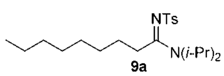 9a	67
10	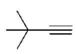	(*i*-Pr)$_2$NH	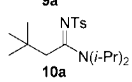 10a	51
11	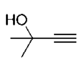	(*i*-Pr)$_2$NH	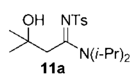 11a	56
12	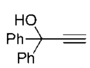	(*i*-Pr)$_2$NH	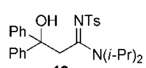 12a	37
13	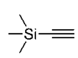	(*i*-Pr)$_2$NH	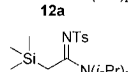 13a	64
14	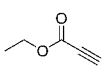	(*i*-Pr)$_2$NH	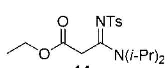 14a	55[b]
15	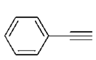	PhNHMe	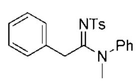 15a	79[c,d]
16	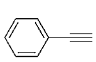	(Ph)$_2$NH	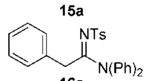 16a	40[c,d]

[a]Reaction conditions: tosylazide, 118 mg, 0.6 mmol; alkynes, 0.5 mmol; amine, 0.6 mmol; MOF−Cu_2I_2(BTTP4), 10 mg, 0.012 mmol; CH_3CN, 1 mL. [b]Triazole (7%) was found. [c]Et_3N (1.2 equiv to alkyne) was added. [d]Run for 6 h.

same initial conversion (less than 5%) in 10 min; however, they led to the completion of 80 and 12%, respectively, in 50 min. At this time, the biggest completion difference of 68% was evident for these two substrates. In contrast, in the presence of CuI, the reactions of PhCCH and *t*-BuCCH displayed almost the same transformation rate, and the reaction with *t*-BuCCH gave slightly higher conversion under the same reaction time. The induction period in the presence of MOF−Cu_2I_2(BTTP4) for the *t*-BuCCH might be due to the slow diffusion of bulky *t*-BuCCH into the pores of the MOF catalyst.

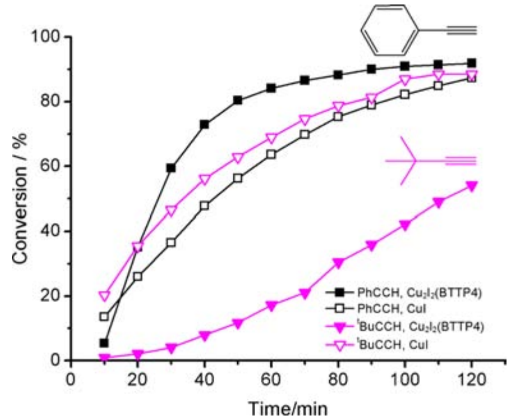

Figure 2. Different catalytic behaviors of CuI and MOF−Cu_2I_2(BTTP4).

Besides the much more obvious size effect of MOF−Cu_2I_2(BTTP4) catalysis compared to that of naked CuI-catalyzed reactions, electronic variation of alkynes caused a big change in the efficiency of the MOF−Cu_2I_2(BTTP4)-catalyzed reactions (entries 4 vs 6). It is noted that the reaction with electron-deficient alkyne ethyl propiolate generates amidine **14a** and tosyltriazone **14b** with 55 and 7% yield, respectively, which was the only case in our system that a minor amount of tosyltriazole was formed (entry 14). With respect to functional group compatibility, a range of functional groups including halide, alcohol, ester, and silyl functional groups were well-tolerated in the MOF−Cu_2I_2(BTTP4)-catalyzed reactions. Amines other than (*i*-Pr)$_2$NH such as *N*-methylaniline (Ph(Me)NH) and diphenylamine (Ph_2NH) have also been tested, and the results showed that the reactivity was in the order of (*i*-Pr)$_2$NH > Ph(Me)NH > Ph_2NH (entries 1, 15, and 16).

To investigate whether the catalytic reactions are heterogeneous or homogeneous, we carried out a filtration experiment (Figure 3). At the 45% conversion of the three-component coupling of Ts−N_3, PhCCH, and (*i*-Pr)$_2$NH in the presence of MOF−Cu_2I_2(BTTP4) for 40 min, the reaction mixture was

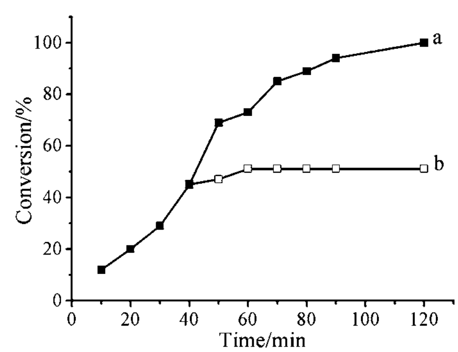

Figure 3. (a) Filtration experiment for MOF−Cu_2I_2(BTTP4). Conversions are given as a function of time. The full square (■) represents the reaction with MOF−Cu_2I_2(BTTP4) as a catalyst. (b) The open square (□) represents the reaction course after filtration of the catalyst at 45% conversion.

separated into two parts. One part of the reaction containing the catalyst was allowed to react for another 80 min until the reaction reached 100% conversion, whereas the remaining part of the reaction was passed through a Celite pad (P4) to remove the catalyst, and the supernatant was allowed to stand for 80 min. Compared to 100% completion for the part of the reaction with the catalyst, it was found that the conversion of the supernatant rose to 51% with only a 6% increase during the same time. Based on the filtration experiment, we believe that the reaction is basically heterogeneous, and we ascribe the additional 6% conversion to the leached copper during the reaction. Inductively coupled plasma optical emission spectrometer analysis of the reaction filtrate indicated that the amount of the copper leaching into the reaction mixture was 3.0% of the total Cu content in the MOF−Cu_2I_2(BTTP4) catalyst, corresponding to 1.888 ppm.

One remarkable feature of this three-component coupling catalysis is that MOF−Cu_2I_2(BTTP4) crystals can be easily isolated from the reaction suspension by simple filtration alone and can be reused at least four times without any loss in yield (Figure 4). As shown in Figure S2, the PXRD patterns recorded

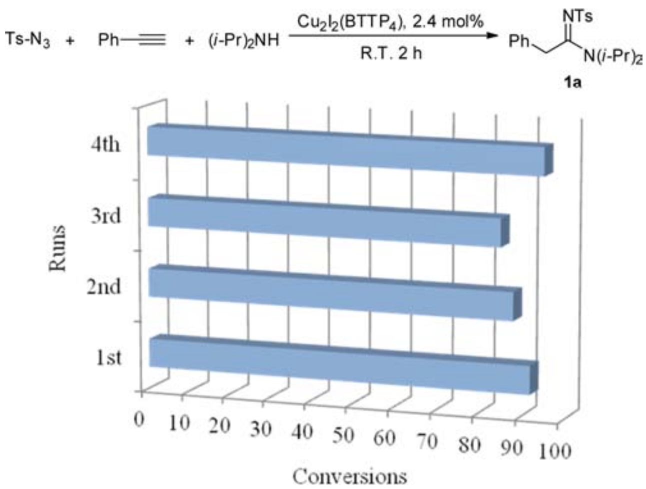

Figure 4. Recycling experiments.

for the recovered catalyst after the four runs showed no signs of framework collapse and decomposition. On the other hand, the XPS spectra displayed the same two intense peaks at 932.8 ± 0.2 and 952.5 ± 0.2 eV assigned to Cu $2p^{3/2}$ and Cu $2p^{1/2}$ components for MOF−Cu_2I_2(BTTP4) catalysts before and after the reaction (Figure S10). These data suggested that both the valence states of the copper before and after the reaction were +1.

3.2. Physical Characterizations of MOF−Cu_2I_2(BTTP4) after Reactions. We measured CO_2 gas adsorption/desorption isotherms for MOF−Cu_2I_2(BTTP4) samples, which were activated under similar conditions before and after catalytic reactions (Figure 5). At 195 K, the amount of CO_2 uptake at 1 atm reach 25.4 and 8.9 wt % before and after catalytic reactions, corresponding to 6.4 and 1.8 CO_2 molecules per Cu_2I_2 unit, respectively. We ascribe the reduction of adsorption capability of CO_2 by MOF−Cu_2I_2(BTTP4) after catalysis to the presence of remaining tosylazide (0.2 equiv excess relative to alkyne) or amidine products that might block the adsorption sites inside the framework pores because the integrity of the porous framework and crystallinity of MOF−Cu_2I_2(BTTP4) catalysts have been proven by PXRD to be well-

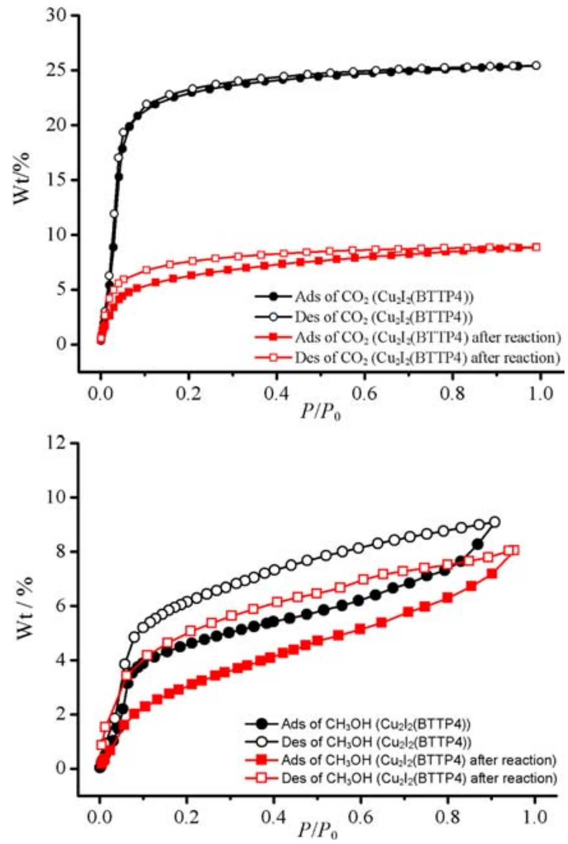

Figure 5. Gas CO_2 (195 K) and vapor CH_3OH (298 K) adsorption/desorption isotherms of MOF−Cu_2I_2(BTTP4) before and after catalytic reactions.

retained after catalytic reactions (Figure S2). On the contrary, the amount of CH_3OH uptake before and after catalytic reactions did not display a big difference and reach 9.1 and 8.0 wt %, corresponding to 2.6 and 2.3 CH_3OH per Cu_2I_2 unit, respectively. This means that although the Cu_2I_2 active sites could be partially shielded by the remaining reactants or products after catalytic reactions, the methanol molecules can still access the framework pores due to the stronger interactions between the pore surface and methanol molecules rather than CO_2 molecules.

Furthermore, we carried out the FT-IR experiments of MOF−Cu_2I_2(BTTP4) before and after catalytic reactions (Figure 6). By simply immersing as-synthesized MOF−Cu_2I_2(BTTP4) crystals in a CH_3CN solution of Ts−N_3 at room temperature for 2 h, the FT-IR spectrum of the solid sample displayed a small peak at 2125 cm^{-1}, confirming the presence of azide (−N_3) in the porous framework. On the other hand, Figure 6 also showed the FT-IR spectrum of MOF−Cu_2I_2(BTTP4) after catalytic reaction. The sharp band at 1541 cm^{-1} was assignable to C═N bending vibration, indicative of the presence of amidine in the MOF−Cu_2I_2(BTTP4) catalyst. Moreover, Ts−N_3 was found in MOF−Cu_2I_2(BTTP4) after catalytic reactions. Based on these results, we proposed that azides entered the framework channels of MOF−Cu_2I_2(BTTP4) and underwent reactions inside the catalyst pores to yield the amidine products.

3.3. In Situ MOF Preparation. Although MOF−Cu_2I_2(BTTP4) displayed much bigger size and greater electronic effects than naked CuI in the three-component coupling reactions, both catalysts were highly effective for

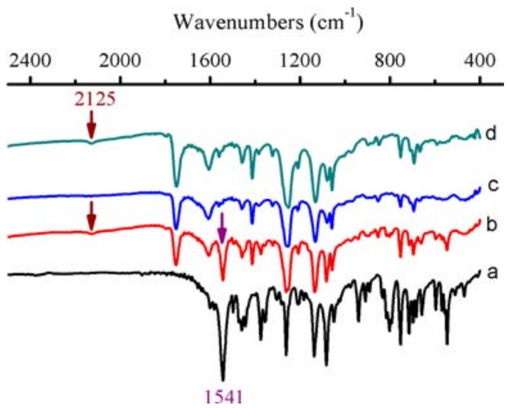

Figure 6. (a) FT-IR of **1a**, (b) samples of MOF−Cu_2I_2(BTTP4) after catalytic reaction, (c) as-prepared MOF−Cu_2I_2(BTTP4), and (d) samples of MOF−Cu_2I_2(BTTP4) immersed in solution of Ts−N_3.

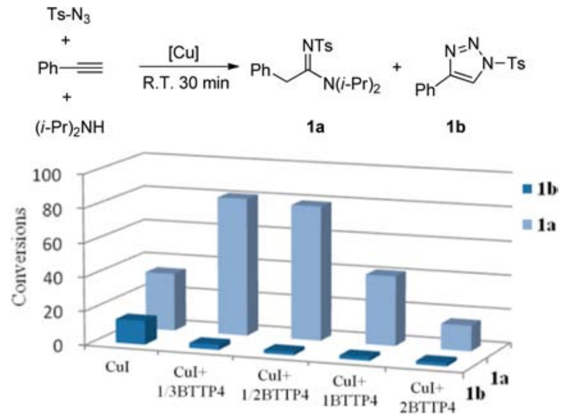

Figure 7. Ligand-accelerated catalytic performances with variable CuI/BTTP4 molar ratios.

aromatic alkynes. On the other hand, it has been well-established by Finn and Fokin that nitrogen-containing ligands such as triazoles, benzimidazoles, and pyridines can display dramatic enhancement in reactivity and selectivity in CuI-catalyzed reactions. To test the effects of the pyridine-based ligand BTTP4 on CuI catalysis of such three-component coupling, we chose the reaction among Ts−N_3, an aromatic alkyne of PhCCH, and (i-Pr)$_2$NH as a model reaction. In the typical procedure for CuI-catalyzed reactions, 10 mol % of CuI was employed, and the reactions were performed under a N_2 atmosphere.[30] To challenge the BTTP4 ligand, a limited amount of CuI (2.4 mol %) was used with no effort to exclude oxygen beyond capping the reaction vial. CuI and BTTP4 were separately dissolved in the corresponding highly soluble solvents of CH_3CN and $CHCl_3$, respectively, and thus, different molar ratios (e.g., 3:1, 2:1, 1:1, and 1:2) of CuI/BTTP4 mixtures have been prepared. It was found that regardless of the varied CuI/BTTP4 ratios, a large amount of orange-yellow crystallites formed rapidly when a CH_3CN solution of CuI was mixed with a $CHCl_3$ solution of $BTTP_4$. After the process of mixing, to the obtained suspension were subsequently added Ts−N_3, PhCCH, and (i-Pr)$_2$NH, and violent bubbling appeared after this addition, indicating the start of the reaction. Until the completion of the reaction, negligible loss of the orange-yellow crystallites was detected.

As shown in Figure 7, the CuI-catalyzed three-component coupling reaction among Ts−N_3, PhCCH, and (i-Pr)$_2$NH leads to the formation of N-sulfonylamidine (**1a**) as the major product and tosyltriazole (**1b**) as the minor one. In the absence of the BTTP4 ligand, the reaction gave less than 40% of **1a** in 30 min at room temperature, whereas the addition of 1/3 or 1/2 of BTTP4 ligand with respect to CuI yielded around 80% of **1a** in the same time and at the same temperature. However, at a CuI/BTTP4 molar ratio of 1:2, the reaction obviously became inhibited, reducing the completion of the reaction down to less than 20%. On the other hand, existence of the BTTP4 ligand can largely enhance the chemoselectivity of this three-component coupling reaction. In the absence of BTTP4, the **1a**/**1b** ratio was 3:1, whereas in the presence of 1/3, 1/2, 1, and 2 equiv of BTTP4, the **1a**/**1b** ratios were 27:1, 40:1, 21:1, and 8:1, respectively. These results suggest that BTTP4 ligand is competent in protecting CuI under the reaction conditions and promoting CuI-catalyzed transformation of the three-component coupling with a noticeable ligand-acceleration effect and chemoselectivity. Nevertheless, it should be noted that the acceleration effect and improved chemoselectivity of BTTP4 was limited in a shorter reaction time (e.g., 30 min). The conversions with a longer reaction time in the presence of naked CuI or the mixtures of CuI/BTTP4 are shown in Figure S3. After 2 h, the CuI-catalyzed reaction accomplished with the same completion values that are approximately 80% of those for CuI/BTTP4 mixtures.

As discussed above, we observed that the catalytic effectiveness relied closely on the molar ratios of CuI/BTTP4, which aroused our interests to analyze the CuI/BTTP4 mixtures and disclose the structures of the in situ formed crystallites at different molar ratios. We measured the PXRD patterns of the solids isolated from suspension of CuI and BTTP4 mixtures with different molar ratios. As depicted in Figure 8, the PXRD patterns of orange solids obtained from

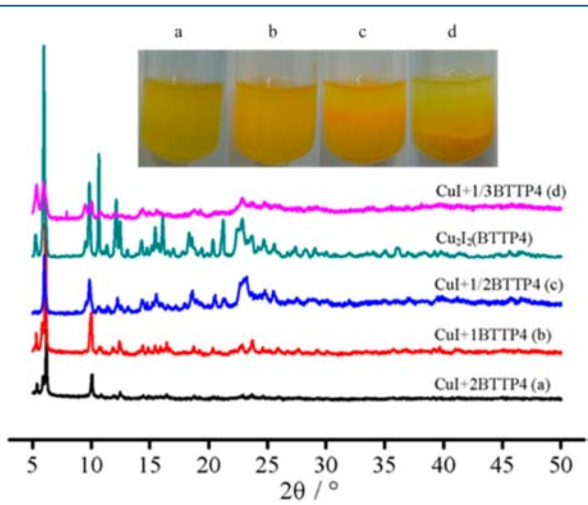

Figure 8. Comparison of the PXRD patterns of as-prepared MOF−Cu_2I_2(BTTP4) with those of the crystallites isolated from suspension of CuI and BTTP4 mixtures with different molar ratios. Inset shows the photos of in situ mixtures.

1:2, 1:1, and 2:1 CuI/BTTP4 mixtures all closely match those of as-synthesized MOF−Cu_2I_2(BTTP4) but with different degrees of crystallinity. The results indicated that a 2:1 CuI/BTTP4 mixture gave the highest relative crystallinity, and the degrees of crystallinity of Cu_2I_2(BTTP4) were in sequence of c (2:1) > b (1:1) > a (1:2). These observations help us believe that the effective catalyst in the mixture was actually the

dx.doi.org/10.1021/ic4012229 | *Inorg. Chem.* 2013, 52, 9053−9059

framework of MOF−Cu_2I_2(BTTP4), regardless of the different CuI/BTTP4 ratios, due to the following reasons: (i) MOF−Cu_2I_2(BTTP4) was the unique product in these solutions in spite of varied CuI/BTTP4 ratios (e.g., 1:2, 1:1, 2:1, and 3:1), whereas the filtrate did not display noticeable catalytic activity with the conversion less than 2.8% after 2 h (Figure S4); (ii) excess CuI in solution (in the case of CuI/BTTP4 ratio of 3:1) contributed little to transformation in comparison with the MOF−Cu_2I_2(BTTP4), which was quantitatively formed in the case of the 2:1 CuI/BTTP4 ratio; and (iii) an excess amount of BTTP4 (in cases of CuI/BTTP4 ratios of 1:1 and 1:2) showed an inhibiting effect on reactions probably because they not only prevented the substrates from approximating the active metal centers of MOF−Cu_2I_2(BTTP4), but the 1:1 and 1:2 CuI/BTTP4 mixtures also gave a lower relative crystallinity compared to 2:1 CuI/BTTP4 mixtures.

4. CONCLUSIONS

In summary, the permanently porous metal−organic framework, MOF−Cu_2I_2(BTTP4), which is assembled from a rigid tritopic ligand benzene-1,3,5-triyl triisonicotinate (BTTP4) and CuI, is proven to be able to catalyze the three-component coupling of sulfonyl azides, alkynes, and amines in an efficiently heterogeneous way, leading to formation of important organic compounds of amidines with good yields. The unique structural features of MOF−Cu_2I_2(BTTP4), including incorporation of redox-active and coordinatively unsaturated CuI sites into pore surface, suitable framework channel size surrounded by rigid nitrogen-containing tripodal ligands, and porosity robustness against evacuation of solvent molecules, endow the MOF−Cu_2I_2(BTTP4) catalyst with versatile character such as unprecedented heterogeneous ligand-accelerated effect, size-effect, and recyclability for reuse of the catalyst. The catalytic performance has been studied by various physical and chemical methods, indicating that MOF−Cu_2I_2(BTTP4) could provide a platform to carry out the catalytic reactions inside its large cavities. Further investigations on the catalytic applications of MOF−Cu_2I_2(BTTP4) toward more organic reactions are underway.

■ ASSOCIATED CONTENT

Ⓢ Supporting Information

Ligand-accelerated catalytic experiments, catalytic recycle test, synthesis of Ts−N_3, NMR spectra of pure products of amidines, and single-crystal and powder X-ray diffraction (PXRD) analyses. This material is available free of charge via the Internet at http://pubs.acs.org.

■ AUTHOR INFORMATION

Corresponding Author

*E-mail: zhli99@mail.sysu.edu.cn (L.Z.), cesscy@mail.sysu.edu.cn (C.-Y.S.).

Notes

The authors declare no competing financial interest.

■ ACKNOWLEDGMENTS

This work was supported by the 973 Program (2012CB821701) and NSF Projects (21102186, 91222201, 21121061, 21173272, and U0934003) of China, the FRF for the Central Universities, and the RFDP of Higher Education of China.

■ REFERENCES

(1) Farrusseng, D.; Aguado, S.; Pinel, C. *Angew. Chem., Int. Ed.* **2009**, *48*, 7502−7513.
(2) Ma, L.; Abney, C.; Lin, W. *Chem. Soc. Rev.* **2009**, *38*, 1248−1256.
(3) Lee, J. Y.; Farha, O. K.; Roberts, J.; Scheidt, K. A.; Nguyen, S. B. T.; Hupp, J. T. *Chem. Soc. Rev.* **2009**, *38*, 1450−1459.
(4) (a) Corma, A.; García, H.; LIabrés i Xamena, F. X. *Chem. Rev.* **2010**, *110*, 4606−4655. (b) Dhakshinamoorthy, A.; García, H. *Chem. Soc. Rev.* **2012**, *41*, 5262−5284.
(5) Kim, K.; Banerjee, M.; Yoon, M.; Das, S. *Top. Curr. Chem.* **2010**, *293*, 115−153.
(6) Ma, L.; Lin, W. *Top. Curr. Chem.* **2010**, *293*, 175−205.
(7) Yoon, M.; Srirambalaji, R.; Kim, K. *Chem. Rev.* **2012**, *112*, 1196−1231.
(8) (a) Huang, Y.; Liu, T.; Lin, J.; Lü, J.; Lin, Z.; Cao, R. *Inorg. Chem.* **2011**, *50*, 2191−2198. (b) Huang, Y.; Lin, Z.; Cao, R. *Chem.—Eur. J.* **2011**, *17*, 12706−12712. (c) Huang, Y.; Liu, S.; Lin, Z.; Li, W.; Li, X.; Cao, R. *J. Catal.* **2012**, *292*, 111−117.
(9) Falkowski, J. M.; Wang, C.; Liu, S.; Lin, W. *Angew. Chem., Int. Ed.* **2011**, *50*, 8674−8678.
(10) Farha, O. K.; Shultz, A. M.; Sarjeant, A. A.; Nguyen, S. T.; Hupp, J. T. *J. Am. Chem. Soc.* **2011**, *133*, 5652−5655.
(11) Yang, X.-L.; Xie, M.-H.; Zou, C.; He, Y.; Chen, B.; O'Keeffe, M.; Wu, C.-D. *J. Am. Chem. Soc.* **2012**, *134*, 10638−10645.
(12) Lun, D. J.; Waterhouse, G. I. N.; Telfer, S. G. *J. Am. Chem. Soc.* **2011**, *133*, 5806−5809.
(13) Roberts, J. M.; Fini, B. M.; Sarjeant, A. A.; Farha, O. K.; Hupp, J. T.; Scheidt, K. A. *J. Am. Chem. Soc.* **2012**, *134*, 3334−3337.
(14) Banerjee, M.; Das, S.; Yoon, M.; Choi, H. J.; Hyun, M. H.; Park, S. M.; Seo, G.; Kim, K. *J. Am. Chem. Soc.* **2009**, *131*, 7524−7525.
(15) Wu, P.; He, C.; Wang, J.; Peng, X.; Li, X.; An, Y.; Duan, C. *J. Am. Chem. Soc.* **2012**, *134*, 14991−14999.
(16) Wang, M.; Xie, M.-H.; Wu, C.-D.; Wang, Y.-G. *Chem. Commun.* **2009**, *45*, 2396−2398.
(17) Jing, X.; He, C.; Dong, D.; Yang, L.; Duan, C. *Angew. Chem., Int. Ed.* **2012**, *51*, 10127−10131.
(18) Luz, I.; LIabrés i Xamena, F. X.; Corma, A. *J. Catal.* **2010**, *285*, 285−291.
(19) Jiang, D.; Mallat, T.; Meier, D. M.; Urakawa, A.; Baiker, A. *J. Catal.* **2010**, *270*, 26−33.
(20) Dhakshinamoorthy, A.; Alvaro, M.; Garcia, H. *J. Catal.* **2012**, *289*, 259.
(21) Lin, X.-M.; Li, T.-T.; Chen, L.-F.; Zhang, L.; Su, C.-Y. *Dalton Trans.* **2012**, *41*, 10422−10429.
(22) Lin, X.-M.; Li, T.-T.; Wang, Y.-W.; Zhang, L.; Su, C.-Y. *Chem.—Asian J.* **2012**, *7*, 2796−2804.
(23) Tan, X.; Li, L.; Zhang, J.; Han, X.; Jiang, L.; Li, F.; Su, C.-Y. *Chem. Mater.* **2012**, *24*, 480−485.
(24) Wang, S. J.; Li, L.; Zhang, J. Y.; Yuan, X. C.; Su, C.-Y. *J. Mater. Chem.* **2011**, *21*, 7098−7104.
(25) Yang, R.; Li, L.; Xiong, Y.; Li, J.-R.; Zhou, H.-C.; Su, C.-Y. *Chem.—Asian J.* **2010**, *5*, 2358−2368.
(26) He, Q.-T.; Li, X.-P.; Chen, L.-F.; Zhang, L.; Wang, W.; Su, C.-Y. *ACS Catal.* **2012**, *3*, 1−9.
(27) He, Q.-T.; Li, X.-P.; Liu, Y.; Yu, Z.-Q.; Wang, W.; Su, C.-Y. *Angew. Chem., Int. Ed.* **2009**, *48*, 6156−6159.
(28) Tornøe, C. W.; Christensen, C.; Meldal, M. *J. Org. Chem.* **2002**, *67*, 3057−3064.
(29) Rostovsev, V. V.; Green, L. G.; Fokin, V. V.; Sharpless, K. B. *Angew. Chem., Int. Ed.* **2002**, *41*, 2596−2599.
(30) Bae, I.; Han, H.; Chang, S. *J. Am. Chem. Soc.* **2005**, *127*, 2038−2039.
(31) Cho, S. H.; Yoo, E. J.; Bae, I.; Chang, S. *J. Am. Chem. Soc.* **2005**, *127*, 16046−16047.
(32) Kim, S. H.; Park, S. H.; Choi, J. H.; Chang, S. *Chem.—Asian J.* **2011**, *6*, 2618−2634.
(33) Yoo, E. J.; Chang, S. *Curr. Org. Chem.* **2009**, *13*, 1766−1776.
(34) Rodionov, V. O.; Presolski, S. I.; Gardinier, S.; Lim, Y.-H.; Finn, M. G. *J. Am. Chem. Soc.* **2007**, *129*, 12696−12704.

(35) Presolski, S. I.; Hong, V.; Cho, S.-H.; Finn, M. G. *J. Am. Chem. Soc.* **2010**, *132*, 14570−14576.
(36) Yoo, E. J.; Ahlquist, M.; Kim, S. H.; Bae, I.; Fokin, V. V.; Sharpless, K. B.; Chang, S. *Angew. Chem., Int. Ed.* **2007**, *46*, 1730−1733.